The RF Modelling of a Ku-band Multi-port Amplifier

P. James

Airbus Defence and Space (UK) Ltd, Portsmouth, Hampshire, PO3 5PU, UK

Abstract — The object of this paper is to describe the RF modelling of a Ku-band MPA. This has been performed to compare against the measured results of an MPA demonstrator that has been designed, constructed and tested at Airbus. It will describe the modelling process and show some predicted and measured results. The model may then be used for predictions in the future prior to the construction and measurement of a real flight MPA. In addition it becomes a generic model from which future models may be based upon.

I. Introduction

An MPA is used to amplify signals with usually 8 input and 8 output ports, although designs with other numbers are possible, fig 1, [1]. It comprises of a power divider or INET, amplifiers in the form of Linearised TWTAs and a power combiner ONET, [2, 3]. In addition it will consist of a switch redundancy network enabling a spare amplifier to be substituted in the event of a potential failure. The aim of this paper is to show how the RF modelling has been performed, to present some predictions and finally to show some measured results from the Ku-band MPA demonstrator.

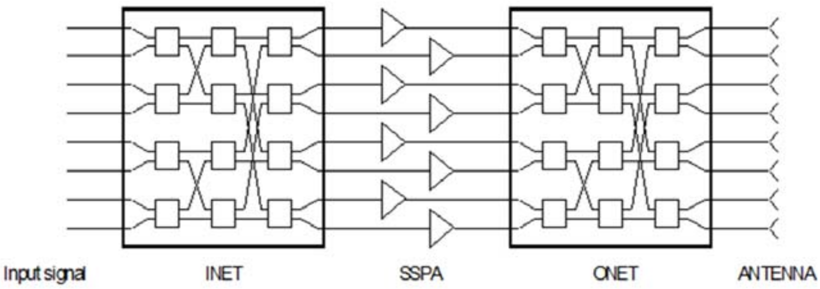

Fig. 1 The MPA showing the amplifiers and matrix networks

II. MODEL OVERVIEW

An MPA can amplify up to 8 input signals .It achieves this by splitting the incoming signals 8 ways within an INET, amplifying these quadrature and 180° phase signals and recombining them within an ONET, [4,5]. The MPA comprises of a waveguide INET and ONET designed to mimic the ideal combiner/divider as near as possible in terms of phase and amplitude response with respect to frequency. It achieves this through a set of E & H plane waveguide hybrid couplers. Waveguide switches allow for a redundant amplifier to be used in the event of a failure. Compensation loops must be incorporated into the switch network to allow for all paths to be of equal phase. Fixed select on test attenuators and line stretchers allow for initial phase and amplitude alignment. Linearized TWTAs are located within each path and comprise an electronically controlled attenuator and phase adjuster. Waveguide is the natural choice for the transmission line within the high power transmission lines whilst a mixture of waveguide and coaxial cable are implemented within the low power section. Isolators are place both before and after the amplifiers to provide for additional matching within the overall circuit.

The MPA has the potential to amplify a signal eight times above what a conventional amplifier could accomplish. There are however a couple of limitations to the MPA concept in practice. First a given single input signal on any input port will give rise to an output signal on one output port and relatively low level signals on the other 7 output ports. These additional signals are due to phase and amplitude errors within the MPA itself, causing the signals to recombine incorrectly within the ONET combiner. This effect gives rise to degraded output port isolation and inevitably cross-talk within the amplified signals. It may be minimised by effective gain and phase control within the MPA, [6]. A second limitation is the need to operate each of the amplifiers in output back-off (OBO) mode. This is to minimise the spectral leakage of intermodulation signals generated by the amplifiers when they are operated in multicarrier mode. Typically they would be operated at an OBO. Any model of the MPA should ideally be able to operate with a multiple of continuous wave signals or with representative modulated signals. It should be able to predict the output isolation as well as carrier to noise ratio, C/Im.

II. MPA METHODOLOGY

Operation of the MPA can be understood more clearly if the INET and ONET matrices are expressed as **A** and the amplifiers by the diagonal matrix **S** and phase and amplitude errors defined as the diagonal matrix **E**. If a single signal of unity amplitude is defined as:

$$\mathbf{Vin} = (1\ 0\ 0\ 0\ 0\ 0\ 0\ 0) \qquad (1)$$

Then the output signals can be expressed in matrix form as:

$$\mathbf{Vout} = \mathbf{A\ S\ E\ A\ Vin}^{\mathbf{T}} \qquad (2)$$

The model includes all these features as well as the non-linear characteristics of the amplifiers. In this way the amplified signals and the leakage signals onto the other output ports may be predicted.

III. MODEL IMPLEMENTATION

A computer model was constructed using the ‘Keysight ADS’ software which incorporated all the features described previously. The model used measured data wherever possible such as for the INET, ONET and amplifiers. The INET and ONET are identical waveguide structures and for each, separate measured models were incorporated into the overall MPA model. Whilst the amplifiers were designed to have similar performance their separate measured data files were included within the MPA model, fig2. In this way the results from the model should be able to have good agreement with the measurements. Different types of signals may be injected into the model. A single CW signal swept over a range of powers would allow the saturation of the MPA to be seen. Also, multiple signal tones of different frequencies would allow for the intermodulation signals to be observed as a spectrum. A simple CW signal swept over the frequency band will allow the isolation versus frequency to be obtained. Modulated signals are more representative of traffic and allow the carrier to noise ratio to be calculated from the amplified spectra. Noise can be injected into the model to predict noise power ratio.

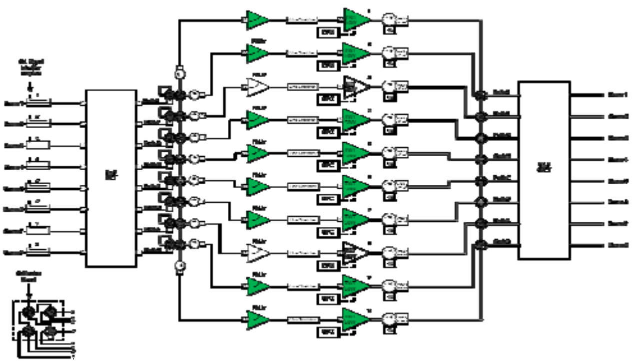

Fig. 2   The MPA showing the amplifiers and redundancy network

IIII. RESULTS

The model was simulated for a CW signal injected into an input port and the signal power was varied to be able to observe the predicted and measured saturation characteristics of the amplifiers within the MPA, fig 3. It may be observed that there is close agreement between measurement and prediction. The predicted and measured output normalized gains vs. frequency are presented in fig 4 and fig 5 respectively. The predicted and measured isolation at output port 5 is shown in fig 6 and fig 7 respectively. It shows that the isolation is better than 25 dB over a bandwidth of 2 GHz for both the prediction from the model and the measurement from the demonstrator which is a very encouraging result. A histogram of predicted and measured MPA isolation is shown in fig 8. It may be observed that there is very close agreement between the measured and predicted curves. A histogram of predicted and measured aggregate MPA isolation is shown in fig 9. Reasonable agreement between prediction and measurement has been attained for aggregate isolation.

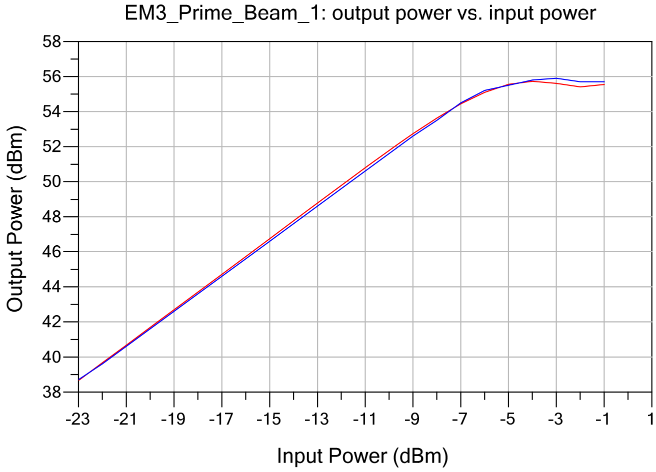

Fig 3 Output power vs. input power for the MPA (measured red, predicted blue)

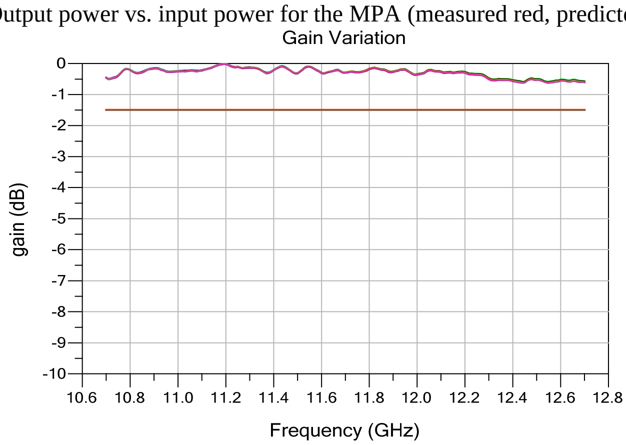

Fig 4 Predicted gain variation vs. frequency

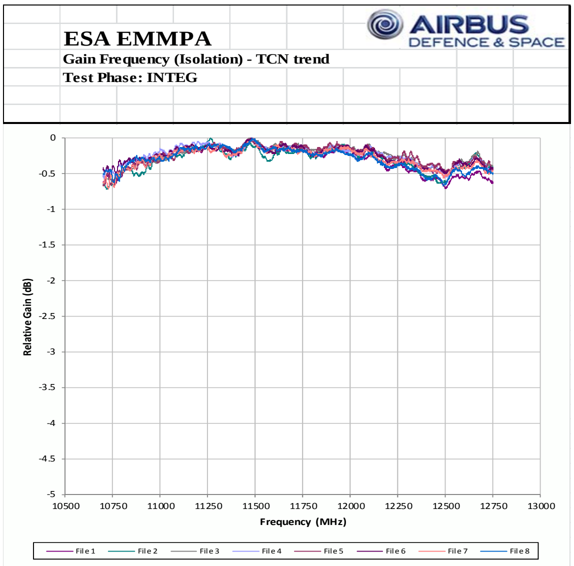

Fig 5 Measured gain variation vs. frequency

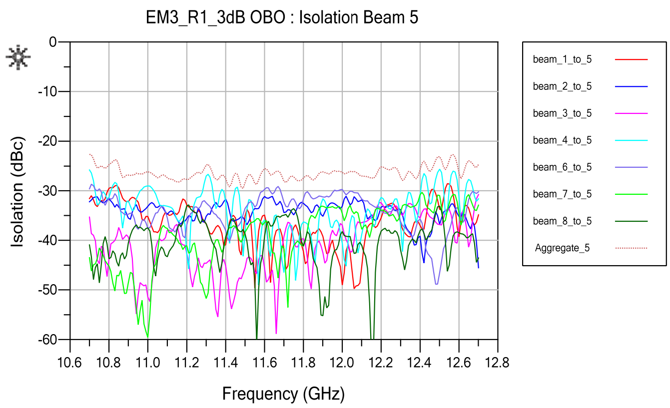

Fig 6 Predicted MPA isolation vs. frequency

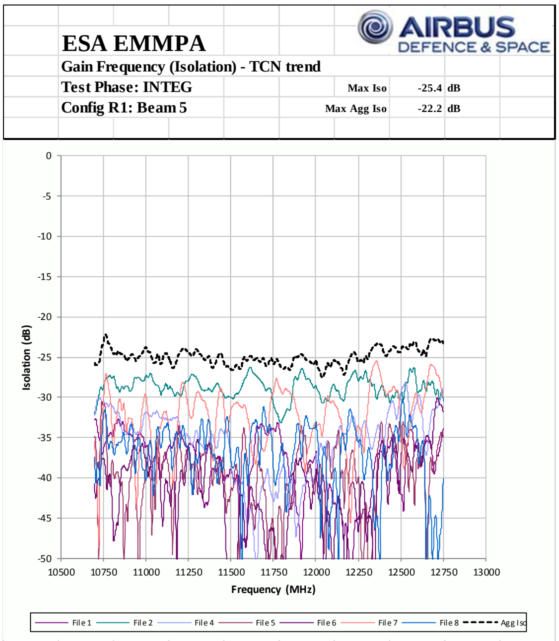

Fig 7 Measured MPA isolation vs. frequency

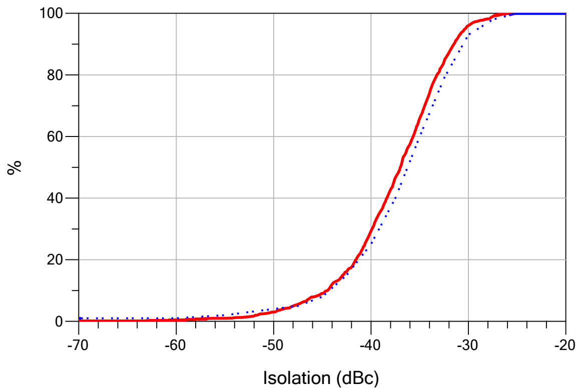

Fig 8 Histogram of predicted (red) and measured (blue) MPA isolation

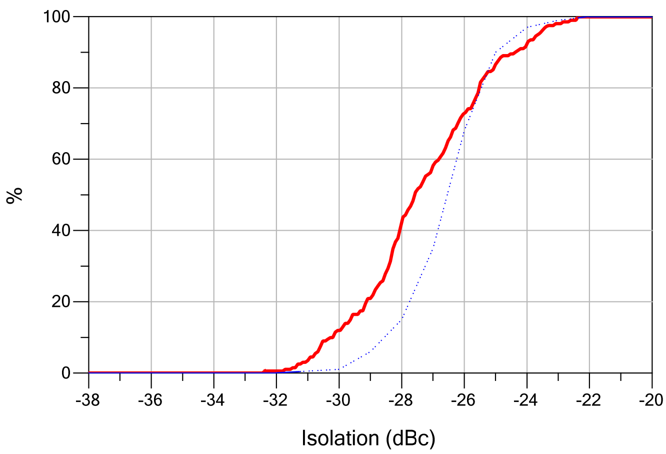

Fig 9 Histogram of predicted (red) and measured (blue) aggregate MPA isolation

A simulation of the intermodulation was performed by injecting two signal tones into one input port and observing the output amplified signals. The C/Im versus Input Back-Off for both prediction and measurement is presented in fig 10. Rather good correlation between measurement and prediction is shown here. In addition it shows the need to operate the MPA at back-off rather than at saturation.

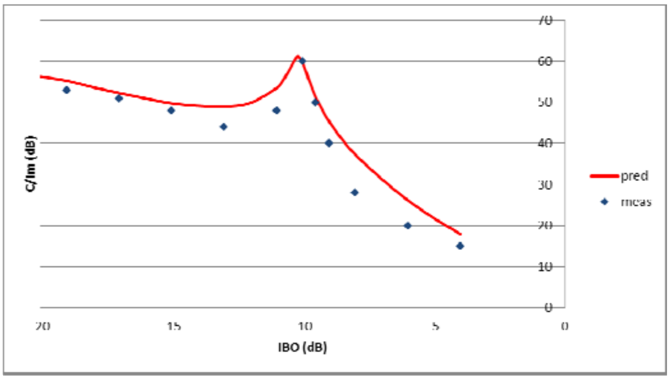

Fig 10 C/Im vs. IBO for prediction (red) and measurement (blue)

By injecting noise with a narrow band notch the noise power ratio has been calculated. Good agreement between measurement and prediction has been obtained. Finally the MPA is shown in fig 12 in the Portsmouth cleanroom.

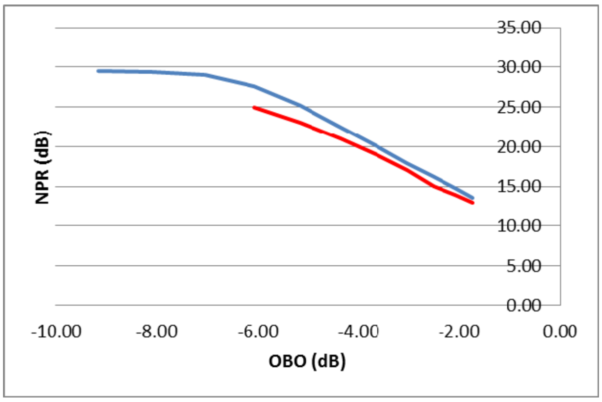

Fig 11 Noise power ratio vs. Output Back-Off, prediction (red) and measurement (blue)

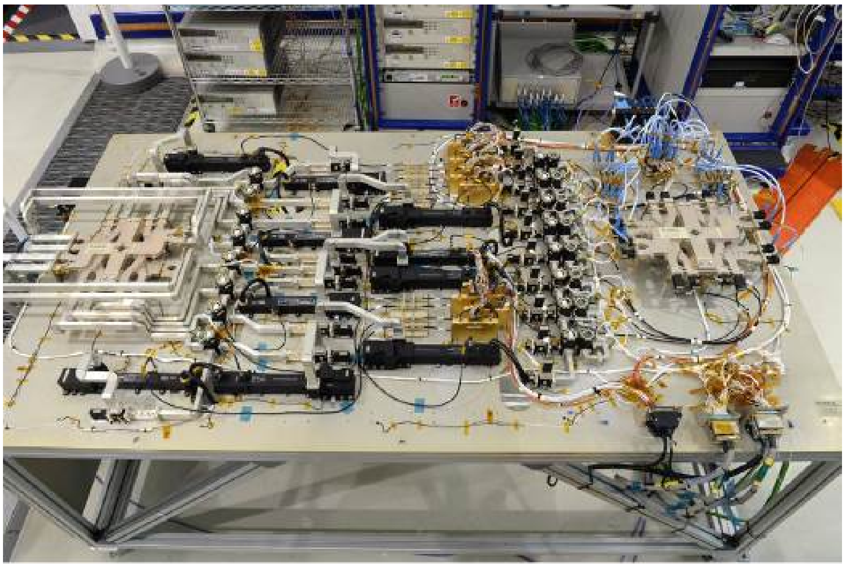

Fig 12 EM MPA in the Portsmouth cleanroom [7]

VI. CONCLUSION

This paper has described the RF modelling of a Multi-Port Amplifier suitable for Ku-band space applications. It has been developed using the ‘Keysight’ ‘ADS’ software. It has described the detailed modelling process and has presented some predictions. These predictions have been compared with measured results from a Ku-band MPA demonstrator and have shown to have good correlation which is very encouraging. It has shown that an MPA model can be used with confidence for RF predictions prior to the building of a flight MPA. In the modelling process the placement of the different components has been done with a view to making the MPA model generic in nature. In this way the model of the 8x8 MPA for a demonstrator may be seen as a precursor for a flight MPA. Thus a flight MPA model will give enhanced confidence.

VI. REFERENCES

[1] The Butler Matrix Transponder’, Comsat Tech. Rev., vol. 4. no.2, pp. 319-345, Fall 1974. W. A. Sandrin

[2] Design of a Multiport Amplifier Beam Forming Network for a Mobile Communications Antenna, J. Lowdell, S. V. Potter, P.James, G. Cobb, M.Walden & R. Hopper. EuCap Nice, Nov 2006.

[3] RF Modelling of a Multiport Amplifier for a Mobile Communications Satellite’, P. James, S.V. Potter, G. R. Cobb & M. Walden, ARMMS, 2007.

[4] RF Modelling and Hardware Realisation of Input and Output Networks for use in a Multiport Amplifier Configuration. A. Pratt. ARMMS 2015.

[5] Detailed Design of a Generic Ka-band Multi Port Amplifier 4, P.James, D. Daryanani O. Clarke & M. Connolly, 2012, 2nd ESA Workshop on Advanced Flexible Telecom Payloads.

[6] The Optimisation of a Multiport Amplifier using an Evolutionary Relaxation Method, P.James European Microwave Conference, Manchester, UK, Sept 2006.

[7] Measured Performance of an Engineering Model Ku-band Multiport Amplifier, 3rd ESA Workshop on Advanced Flexible Telecom Payloads, T. Watson, N. Wheatley, M.Harverson, F. Coromina. March 2016, ESA/ESTEC

VII. Acknowledgements

The author would like to thank the European Space Agency for their help and assistance in this work. This work has been performed under a programme of and funded by the European Space Agency (ARTES Competitiveness & Growth).
The view expressed herein can in no way be taken to reflect the official opinion of the European Space Agency.